

NATIONAL ADVISORY COMMITTEE FOR AERONAUTICS

TECHNICAL NOTE

No. 1739

COMPARISON WITH EXPERIMENT OF SEVERAL METHODS
OF PREDICTING THE LIFT OF WINGS IN
SUBSONIC COMPRESSIBLE FLOW

By Harry E. Murray

Langley Aeronautical Laboratory
Langley Field, Va.



Washington

October 1948

DISTRIBUTION STATEMENT A
Approved for Public Release
Distribution Unlimited

Reproduced From
Best Available Copy

20000807 201

EMC QUALITY INSPECTED 4

AQM00-11-3603

NATIONAL ADVISORY COMMITTEE FOR AERONAUTICS

TECHNICAL NOTE NO. 1739

COMPARISON WITH EXPERIMENT OF SEVERAL METHODS
OF PREDICTING THE LIFT OF WINGS IN
SUBSONIC COMPRESSIBLE FLOW

By Harry E. Murray

SUMMARY

Several methods of predicting the lift of wings in subsonic compressible flow were compared with experiment. An experimental verification of Kaplan's formula for the effect of compressibility on the lift of wing sections was obtained.

Semiempirical formulas were developed for predicting the subsonic effects of compressibility on the lift of finite-span wings based on corrections to the section lift-curve slope. These semiempirical formulas yielded better agreement with experiment than previously derived theoretical methods. The agreement at small sweep angles was slightly better when thickness was considered in the semiempirical formulas.

Both experiments and calculations indicated a decrease in the variation of lift with Mach number for increasing sweep.

INTRODUCTION

The effect of compressibility on the lift of finite-span wings has been extensively discussed in previous papers (references 1, 2, and 3, for example). These papers discuss compressibility effects in terms of an affine transformation based on small-perturbation theory herein referred to as the three-dimensional Prandtl transformation. The application of the three-dimensional Prandtl transformation to the lifting-line theory of unswept wings is discussed in references 1 and 2. An application of Weissinger's approximate lifting-surface theory of wings of arbitrary sweep (reference 4) is discussed in reference 3. When compared with experiment, these existing methods did not yield entirely satisfactory results.

Kaplan (reference 5) has shown that including the thickness of a two-dimensional airfoil in calculations of the effect of compressibility on the lift results in appreciable effect at high subsonic Mach numbers.

Inclusion of thickness in the three-dimensional case consequently may also have an appreciable effect. Rather formidable mathematical difficulties are encountered in any rigorous attempt to consider the thickness of a finite-span wing in subsonic compressible flow. To attempt an approximate adaptation of Kaplan's two-dimensional solution to finite-span wings therefore seems reasonable. In the present paper such an approximate adaptation of Kaplan's results to swept and unswept wings is obtained. The method is based on lifting-surface theory (reference 6). Available test data are compared with the present method, as well as with several other methods which neglect the effect of airfoil thickness.

SYMBOLS

C_L	finite-span-wing lift coefficient	$\left(\frac{\text{Lift}}{\frac{\rho}{2} V^2} \right)$
c_l	section lift coefficient	$\left(\frac{\text{Lift per unit span}}{\frac{\rho}{2} c V^2} \right)$
ρ	air mass density	
S	wing area	
c	wing chord	
V	free-stream velocity	
α	angle of attack	
$C_{L\alpha}$	$= \frac{\partial C_L}{\partial \alpha}$	
a_i	section lift-curve slope at $M = 0$	$\left(\frac{\partial c_l}{\partial \alpha} \right)$
a_c	section lift-curve slope at Mach number of M	
M	Mach number	$\left(\frac{V}{\text{Velocity of sound}} \right)$
Λ	sweep angle of wing quarter-chord line, positive for sweepback	
M_e	$= M \cos \Lambda$	

$$\mu = \frac{1}{\sqrt{1 - M^2}}$$

$$\mu_A = \frac{1}{\sqrt{1 - M_e^2}}$$

$$\beta = \sqrt{1 - M^2}$$

$$\beta_K = \frac{1}{\mu + \frac{1}{2}(1 - e^{-2\lambda}) \left[\mu(\mu - 1) + \frac{1}{4}(\gamma + 1)(\mu^2 - 1)^2 \right]}$$

γ ratio of specific heats (1.4 for air)

λ airfoil thickness parameter (ψ_0 in reference 7)

A aspect ratio

$$A_c = A\sqrt{1 - M^2}$$

E_e lifting-surface-theory correction factor based on A

E_{e_c} equivalent value of E_e based on A_c

$$\Lambda_c = \tan^{-1} \frac{\tan \Lambda}{\sqrt{1 - M^2}}$$

F_Λ sweep factor

$$K = a_i F_\Lambda$$

ANALYSIS

The Lift of Two-Dimensional Wings

Kaplan (reference 5) has presented a method whereby the effect of airfoil thickness can be considered in the calculation of the lift of a two-dimensional wing at an angle of attack. Kaplan's formula for the effect of compressibility on lift is

$$\frac{1}{\beta_K} = \frac{a_c}{a_i} = \mu + \frac{1}{2}(1 - e^{-2\lambda}) \left[\mu(\mu - 1) + \frac{1}{4}(\gamma + 1)(\mu^2 - 1)^2 \right] \quad (1)$$

The effect of thickness is included in this formula by means of the parameter λ which relates the chord of the airfoil to the radius of

the conformal circle in Theodorsen's potential theory of arbitrary profiles (reference 7). As the airfoil thickness approaches zero, λ approaches zero and Kaplan's formula can be seen to approach the Prandtl (or Glauert) factor, which is

$$\frac{1}{\beta} = \mu = \frac{1}{\sqrt{1 - M^2}} \quad (2)$$

The variations of section lift-curve slope with Mach number for the NACA 66,1-115 airfoil and for the same airfoil with a beveled trailing edge (models 1 and 2, table I) are shown in figures 1 and 2, respectively (from reference 8). Calculations applying Kaplan's formula (equation (1)) and the Prandtl factor (equation (2)) are also shown for comparison. The short vertical lines on the curves of figures 1 and 2 indicate the lower limit of the test data below which the experimental curve is extrapolated to zero Mach number. Consideration of the thickness (the Kaplan method) improves the agreement between theory and experiment. Similar agreement is shown in figure 3 for an airfoil approximating the NACA 0012-64 airfoil, designated as R-0009 in reference 9, at zero sweep (velocity of free stream normal to wing span).

In reference 10, Jones indicated that the effect of compressibility on a swept two-dimensional wing is the same as on an unswept wing in a stream of reduced Mach number M_e , where

$$M_e = M \cos \Lambda \quad (3)$$

Kaplan's formula can thus be adapted directly to the two-dimensional swept wing by replacing μ by

$$\mu_\Lambda = \frac{1}{\sqrt{1 - M_e^2}} = \frac{1}{\sqrt{1 - M^2 \cos^2 \Lambda}} \quad (4)$$

Calculations made with this modification of Kaplan's formula, together with experimental data and calculations made with the Prandtl correction, are presented in figure 3 for the two-dimensional NACA 0012-64 airfoil (model 3, table I) at three angles of sweep. The results indicate that the foregoing method of predicting the effect of compressibility on a two-dimensional swept wing produces good agreement with experiment for $\Lambda = 20^\circ$ when thickness is considered. The reason for the somewhat poorer agreement for $\Lambda = 40^\circ$ is not known.

Below the short vertical lines on the curves of figures 1, 2, and 3 the experimental curve is extrapolated to zero Mach number by means of Kaplan's formula in which μ_Λ is used.

The Lift of Three-Dimensional Wings

The effect of compressibility on the lift of three-dimensional wings is calculated by four different methods. All four methods stem from the three-dimensional Prandtl transformation. According to the three-dimensional Prandtl transformation as set forth in reference 3, the effect of compressibility on lift can be obtained by increasing by the factor $\frac{1}{\sqrt{1 - M^2}}$ the lift for incompressible flow of wings having equivalent aspect ratios given by

$$A_C = A\sqrt{1 - M^2}$$

and equivalent sweep angles given by

$$\tan \Lambda_C = \frac{\tan \Lambda}{\sqrt{1 - M^2}}$$

Methods 1 and 2 are based on an interpretation of the three-dimensional Prandtl transformation, which is strictly correct only for unswept wings of high aspect ratio to which lifting-line theory is applicable. This particular interpretation was adapted for application to wings of moderate aspect ratio with sweep because it afforded a simple, logical means wherein a correction for thickness based on Kaplan's results (reference 5) could be applied. Methods 3 and 4, however, are strict applications of the three-dimensional Prandtl transformation. No logical or practical method could be discovered for adapting a strict application of the three-dimensional Prandtl transformation to the purpose of accounting for the effects of wing thickness.

Method 1.— According to reference 1, if the three-dimensional Prandtl transformation is applied to lifting-line theory, the lift-curve slope of unswept wings is

$$C_{L_a} = \frac{1}{\beta} \frac{A_C a_i}{A_C + a_i \frac{57.3}{\pi}} \quad (5)$$

where $A_C = \beta A$ and $\beta = \sqrt{1 - M^2}$. Equation (5) also can be written as

$$C_{L_a} = \frac{A \frac{a_i}{\beta}}{A + \frac{a_i}{\beta} \frac{57.3}{\pi}} \quad (6)$$

Equation (6) shows, as has already been observed in reference 2, that for lifting-line theory the effect of compressibility can be accounted for by simply using the correct variation of section lift-curve slope with Mach number. Equations (5) and (6) apply rigorously only to the limiting case of unswept wings having very high aspect ratio. According to reference 6, the lift-curve slope of unswept wings in incompressible flow can be obtained more correctly than by lifting-line theory from the following equation

$$C_{L\alpha} = \frac{Aa_1}{AE_e + a_1 \frac{57.3}{\pi}} \quad (7)$$

which is based on lifting-line theory but corrected according to lifting-surface theory. The product AE_e is shown in figure 4. If the effect of compressibility can be assumed to be accounted for by correcting the section lift-curve slope, as in the case of lifting-line theory, then equation (7) can be written as

$$C_{L\alpha} = \frac{A \frac{a_1}{\beta}}{AE_e + \frac{a_1}{\beta} \frac{57.3}{\pi}} \quad (8)$$

Equation (8) is not a strict application of the three-dimensional Prandtl transformation because of the presence of the quantity E_e . The effect of thickness can be approximately introduced into equation (8) as a correction to the section lift-curve slope by substituting β_K for β ; the resulting equation is

$$C_{L\alpha} = \frac{A \frac{a_1}{\beta_K}}{AE_e + \frac{a_1}{\beta_K} \frac{57.3}{\pi}} \quad (9)$$

Reference 11 has shown that the effect of sweep can be approximately accounted for in formulas for the lift-curve slope of unswept finite-span wings by multiplying the section lift-curve slope by the factor $\cos \Lambda$. If some new factor F_Λ is assumed to account exactly for sweep, then equation (9) can be written to include sweep, as follows:

$$C_{L\alpha} = \frac{A \frac{a_1}{\beta_K} F_\Lambda}{AE_e + \frac{a_1}{\beta_K} F_\Lambda \frac{57.3}{\pi}} \quad (10)$$

For a swept wing the results of the two-dimensional analysis will be used to account approximately for the variation of compressibility effect with sweep. For this purpose β_K in equation (10) will be based on μ_A or, in other words, upon the component of Mach number normal to the swept panel. Comparisons of equation (10) with experiment indicated that best agreement resulted when Λ is defined as the sweep of the quarter-chord line and λ , as used in the equation for β_K , corresponds to the airfoil section normal to the quarter-chord line.

Because F_A cannot be accurately evaluated from available theories for all useful values of aspect ratio and sweep, equation (10) is valuable because of its ability to predict the effect of compressibility on a wing for which low-speed experimental data are available. The quantity $a_i F_A$ can be evaluated from the low-speed test condition and is assumed to be independent of Mach number in the subsonic range.

Equation (10) has been applied as herein explained and is compared with experiment in figures 5 to 19 as method 1. The short vertical lines on the curves of figures 5 to 19 indicate the lower limit of the test data below which the experimental curve is extrapolated to zero Mach number by means of method 1.

Method 2.—Method 2, which is identical to method 1 except that $\lambda = 0$, is included in figures 5 to 19 in order to indicate the order of magnitude of the effect introduced by thickness. When $\lambda = 0$, β_K is replaced by β in equation (10), and the resulting equation is

$$C_{L\alpha} = \frac{A \frac{a_i}{\beta} F_A}{AE_e + \frac{a_i}{\beta} F_A \frac{57.3}{\pi}}$$

Method 3.—A strict application of the three-dimensional Prandtl transformation (reference 3) to very thin unswept, or very slightly swept, wings transforms equation (7) to

$$C_{L\alpha} = \frac{1}{\beta} \frac{A_c a_i}{A_c E_{e_c} + a_i \frac{57.3}{\pi}} \quad (11)$$

Equation (11) has been applied as a correction to low-speed test data for wings of less than $\pm 12^\circ$ sweep and is compared with experiment in figures 5 to 11; a_i is evaluated from the low-speed data by method 1. This application is denoted method 3.

Method 4.—The three-dimensional Prandtl transformation can be extended to thin, swept wings by means of Weissinger's approximate lifting-surface theory of reference 4, as explained in reference 3. Lift-curve slopes calculated by Weissinger's method can be obtained from charts in reference 3 for a wide range of sweep angles, aspect ratios, and taper ratios. Because the Weissinger method calculations were obtained for a section lift-curve slope of 2π (the thin-airfoil-theory value), Weissinger's method was not applied as a correction for compressibility to low-speed data. The calculated values are compared directly with experiment in figures 5 to 19 and are denoted method 4.

RESULTS AND DISCUSSION

Comparison of Experiment and Calculation

Four methods have been used to predict the variation of lift-curve slope with Mach number for finite-span wings. Figures 5 to 19 show comparisons between these methods and experimental data obtained from wind-tunnel tests of wing models. Table I contains supplementary information regarding the models and test conditions for the experimental data; this information was obtained from references 8, 9, 12, 13, 14, and unpublished data. Table I indicates that, for models 4 to 18, jet-boundary corrections were either applied or were negligible. All corrections were applied in a similar manner to account for the effects of boundary-induced velocity and blockage. Failure to apply corrections to the data of models 1, 2, and 3 resulted in a slightly excessive increase of lift-curve slope with Mach number at high subsonic Mach numbers. Application of the correction would, in general, improve slightly the agreement between theory and experiment.

Examination of figures 5 to 19 shows that all wing tests and all four methods of calculation yield an increase of lift with Mach number. Theory and experiment are, therefore, in qualitative agreement. Quantitatively, however, the agreement between calculation and experiment is not quite consistent. Such inconsistencies (figs. 8 and 10, for example) are to be expected, however, because all the calculations are based on potential flow. Methods 1, 2, and 3 are applied as corrections to low-speed test data which account for the low-speed boundary-layer effects. If the Reynolds number changes which usually accompany Mach number variation produce variations in the boundary layer of the airfoil, an additional variation of lift-curve slope with Mach number, which is not predictable by the methods discussed herein, will occur. The marked difference between experiment and results calculated by method 4 in figure 6 results from the wing model having a full-span elevator with an overhang and an open gap. When the variation of lift-curve slope with Mach number was calculated by methods 1, 2, and 3, the gap was considered in terms of its effect on the low-speed section lift-curve slope. No consideration of the gap was made when method 4 was applied.

In general, of the four methods, methods 1 and 2 compare most favorably with experiment. Of these two methods, method 1 which includes a consideration of section thickness appears somewhat better than method 2, particularly for small sweep angles. Method 2 gives less increase of lift-curve slope with Mach number than method 1. Method 3 indicates even less increase of lift-curve slope with Mach number than method 2 and seems to be in poorer agreement with experiment. Method 4 indicates an increase of lift-curve slope with Mach number less than method 2 but similar to method 3. Coincidence of the calculations of method 4 and experiment at low Mach numbers was not obtained as was the case with methods 1, 2, and 3 because the calculations were all obtained for a low-speed section lift-curve slope of 2π .

The data of figures 5 to 19, either experimental or calculated, indicate that the variation of lift-curve slope with Mach number decreases as the sweep increases. Furthermore, a comparison of methods 1 and 2 indicates that the effect of thickness upon the variation of lift-curve slope with Mach number decreases with sweep, either positive or negative.

Practical Considerations for Method 1

Because the agreement between experiment and method 1 seemed good, a practical calculation procedure, based on the assumption that a low-speed lift-curve slope is available for the finite-span wing under consideration, is briefly set forth for this method. The constant $a_i F_A$ in equation (10) can be solved for as follows:

$$a_i F_A = \frac{C_{L_\alpha} A E_e \beta_K}{A - C_{L_\alpha} \frac{57.3}{\pi}} = K \quad (12)$$

where C_{L_α} is the value measured at some low Mach number. The quantity $A E_e$ is evaluated from figure 4; whereas β_K is evaluated from equation (1) with μ_A being used rather than μ ; that is, only the component of the Mach number perpendicular to the wing quarter-chord line is considered. The value of K from equation (12) is an effective section lift-curve slope for zero Mach number appropriate to the wing for which the low-speed data were obtained.

The finite-span lift-curve slope and its variation with Mach number for the wing for which K was evaluated can now be written

$$C_{L_\alpha} = \frac{A \frac{K}{\beta_K}}{A E_e + \frac{K}{\beta_K} \frac{57.3}{\pi}} \quad (13)$$

If no low-speed lift-curve slope is available from which to evaluate K , Weissinger's method, which gives $C_{L\alpha}$ at $M = 0$ (charts of reference 3), can be used. If the wing is effectively unswept (sweep angles of quarter-chord line between $\pm 12^\circ$), K approaches a_1 , which can be determined from wing-section tests, many of which are presented in reference 15.

The evaluation of β_K requires that the value of λ be known for the particular airfoil section under consideration. This parameter can, of course, be calculated as explained in reference 7; however, such a calculation is often unnecessary because λ has already been calculated, as a step in the pressure-distribution calculation, for a large number of airfoils. Figure 20 shows the variation of λ with thickness for a number of airfoil series. The value of λ in equation (1) should correspond only to the airfoil basic-thickness form (airfoil without camber). Equation (1) is, therefore, independent of airfoil camber, and figure 20 offers a very wide coverage of airfoils.

As explained in reference 15 there are two slightly differing groups of airfoils both designated as 6-series. The older group shows the low-drag range following a comma after the number denoting the chordwise position of minimum pressure (model 1, table I, for example). A more recent group of airfoils show the low-drag range as a subscript to the number denoting the chordwise position of minimum pressure (model 6, table I, for example). The curves of figure 20 apply only to the latter group of 6-series airfoils.

CONCLUSIONS

A comparison with experiment of several methods of predicting the lift of wings in subsonic compressible flow indicates the following conclusions:

1. Kaplan's formula for the effect of compressibility on the lift of wing sections is in good agreement with experiment.
2. Semiempirical formulas derived for finite-span wings agree with experiment better than previously derived theoretical methods.
3. A slightly better agreement at small sweep angles results from a consideration of thickness in the semiempirical formulas.

4. Both experiments and calculations indicated a decrease in the variation of lift with Mach number for increasing sweep.

Langley Aeronautical Laboratory
National Advisory Committee for Aeronautics
Langley Field, Va., August 6, 1948

REFERENCES

1. Göther, B.: Plane and Three-Dimensional Flow at High Subsonic Speeds. NACA TM No. 1105, 1946.
2. Goldstein, S., and Young, A. D.: The Linear Perturbation Theory of Compressible Flow, with Applications to Wind-Tunnel Interference. R. & M. No. 1909, British A.R.C., 1943.
3. DeYoung, John: Theoretical Additional Span Loading Characteristics of Wings with Arbitrary Sweep, Aspect Ratio, and Taper Ratio. NACA TN No. 1491, 1947.
4. Weissinger, J.: The Lift Distribution of Swept-Back Wings. NACA TM No. 1120, 1947.
5. Kaplan, Carl: Effect of Compressibility at High Subsonic Velocities on the Lifting Force Acting on an Elliptic Cylinder. NACA Rep. No. 834, 1946.
6. Swanson, Robert S., and Crandall, Stewart M.: Lifting-Surface-Theory Aspect-Ratio Corrections to the Lift and Hinge-Moment Parameters for Full-Span Elevators on Horizontal Tail Surfaces. NACA TN No. 1175, 1947.
7. Theodorsen, T., and Garrick, I. E.: General Potential Theory of Arbitrary Wing Sections. NACA Rep. No. 452, 1933.
8. Langley Research Department (Compiled by Thomas A. Toll): Summary of Lateral-Control Research. NACA TN No. 1245, 1947.
9. Lippisch, A., and Beuschausen, W.: Pressure Distribution Measurements at High Speed and Oblique Incidence of Flow. NACA TM No. 1115, 1947.
10. Jones, Robert T.: Wing Plan Forms for High-Speed Flight. NACA TN No. 1033, 1946.
11. Toll, Thomas A., and Queijo, M. J.: Approximate Relations and Charts for Low-Speed Stability Derivatives of Swept Wings. NACA TN No. 1581, 1948.
12. Fischel, Jack, and Schneiter, Leslie E.: High-Speed Wind-Tunnel Investigation of High Lift and Aileron-Control Characteristics of an NACA 65-210 Semispan Wing. NACA TN No. 1473, 1947.
13. Schueler, Carl F., Korycinski, Peter F., and Strass, H. Kurt: Tests of a Full-Scale Horizontal Tail Surface in the Langley 16-Foot High-Speed Tunnel. NACA TN No. 1074, 1946.

14. Pearson, E. O., Jr., Evans, A. J., and West, F. E., Jr.: Effects of Compressibility on the Maximum Lift Characteristics and Spanwise Load Distribution of a 12-Foot-Span Fighter-Type Wing of NACA 230-Series Airfoil Sections. NACA ACR No. 15G10, 1945.
15. Abbott, Ira H., Von Doenhoff, Albert E., and Stivers, Louis S., Jr.: Summary of Airfoil Data. NACA Rep. No. 824, 1945.

TABLE I
SUPPLEMENTARY INFORMATION REGARDING WIND-TUNNEL MODELS AND TESTS

Model	Aspect ratio	Taper ratio	Sweep, Δ (deg)	Airfoil section normal to $\frac{c}{4}$ -line	Reynolds number		λ	Reference	Jet-boundary corrections
					from	to			
1	∞	1	0	NACA 66,1-115	-----	-----	0.1206	8	None
2	∞	1	0	NACA 66,1-115 (modified)	-----	-----	.1235	8	None
3	∞	1	0,20,40	NACA 0012-64 (approx.)	-----	-----	.0812	9	None
4	5.76	.57	0	NACA 65-210	2.0 $\times 10^6$	10.3 $\times 10^6$.0744	12	Corrected
5	4.76	.50	8	NACA 66-009 (approx.)	5.7	14.1	.0670	13	Corrected
6	6.00	.50	0	NACA 65 ₂ -215	5.0	14.0	.1122	Unpublished	Corrected
7	6.00	.50	3.2	NACA 66(215)-116 ¹	3.0	8.0	.1265	Unpublished	Corrected
8	6.00	.50	3.2	NACA 23012	3.0	8.0	.1062	14	Corrected
9	4.65	.56	6.3	NACA 0010-64	4.5	11.0	.0906	Unpublished	Corrected
10	5.36	.31	11.5	NACA 65-010 (approx.)	1.0	4.2	.0740	Unpublished	Corrections negligible
11	5.76	.50	15.0	NACA 65 ₂ -215	5.0	14.0	.1122	Unpublished	Corrected
12	4.78	.50	30.0	NACA 65 ₂ -215	5.0	14.0	.1122	Unpublished	Corrected
13	3.32	.50	45.0	NACA 65 ₂ -215	5.0	14.0	.1122	Unpublished	Corrected
14	2.66	.50	45.0	NACA 65 ₂ -215	5.0	14.0	.1122	Unpublished	Corrected
15	2.31	.27	56.5	NACA 65-010 (approx.)	1.7	7.7	.0740	Unpublished	Corrections negligible
16	3.06	.50	47.8	NACA 65 ₁ -012 (approx.)	4.25	9.25	.0880	Unpublished	Corrected
17	3.01	.60	35.0	NACA 0012-64	2.1	4.9	.1100	Unpublished	Corrected
18	3.00	.31	27.5	NACA 64 ₁ A012 (approx.)	3.5	5.4	.0943	Unpublished	Corrected

¹Variation from NACA 23016 at root to NACA 23009 at tip.



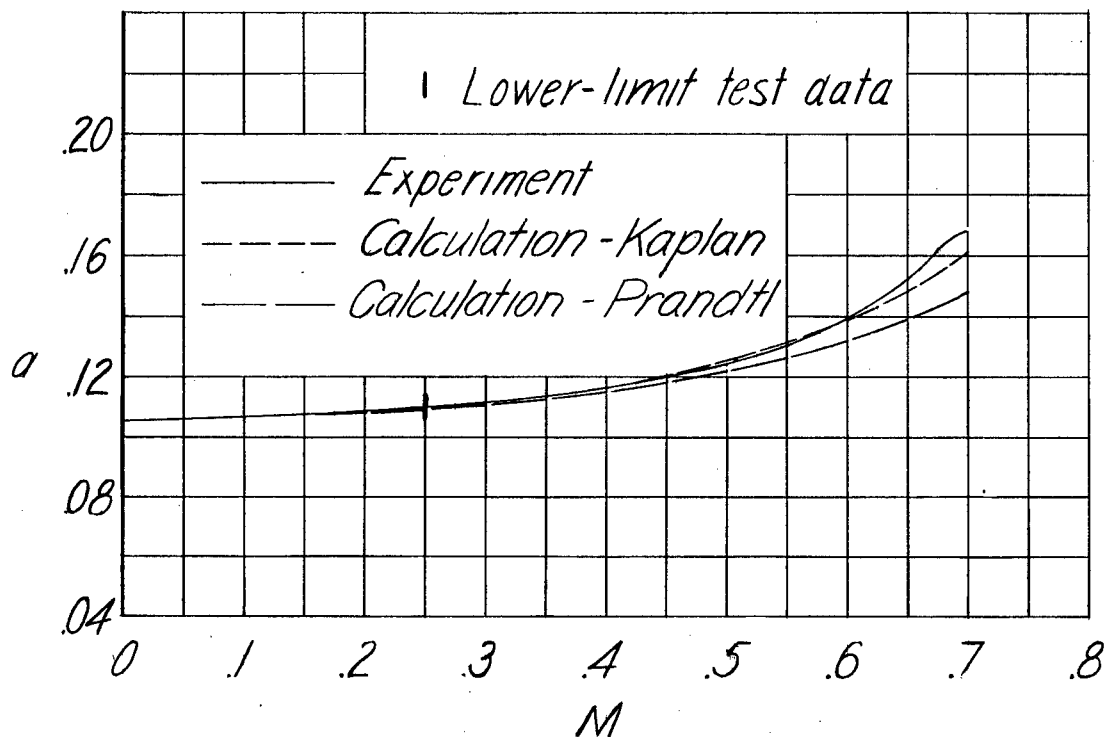


Figure 1.- Variation of two-dimensional lift-curve slope with Mach number. Model 1. $\Lambda = 0^\circ$.

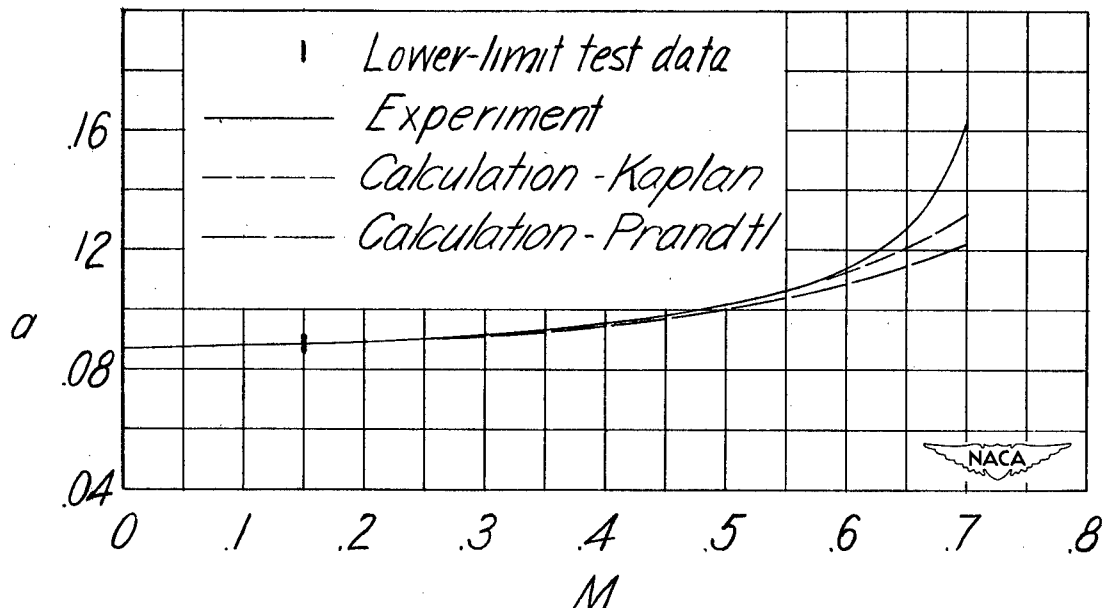


Figure 2.- Variation of two-dimensional lift-curve slope with Mach number. Model 2. $\Lambda = 0^\circ$.

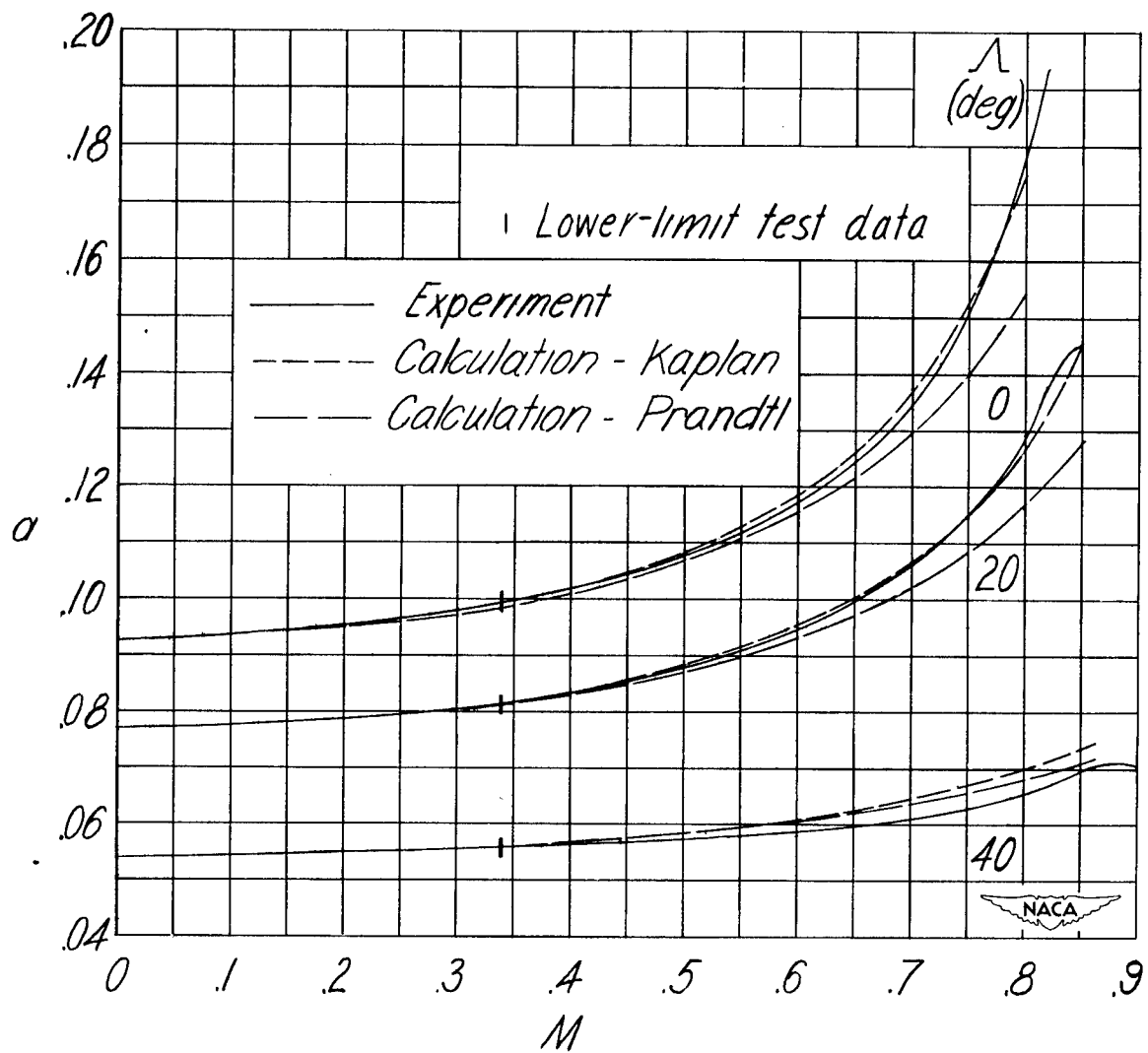


Figure 3.- Variation of two-dimensional lift-curve slope with Mach number for three angles of sweep. Model 3.

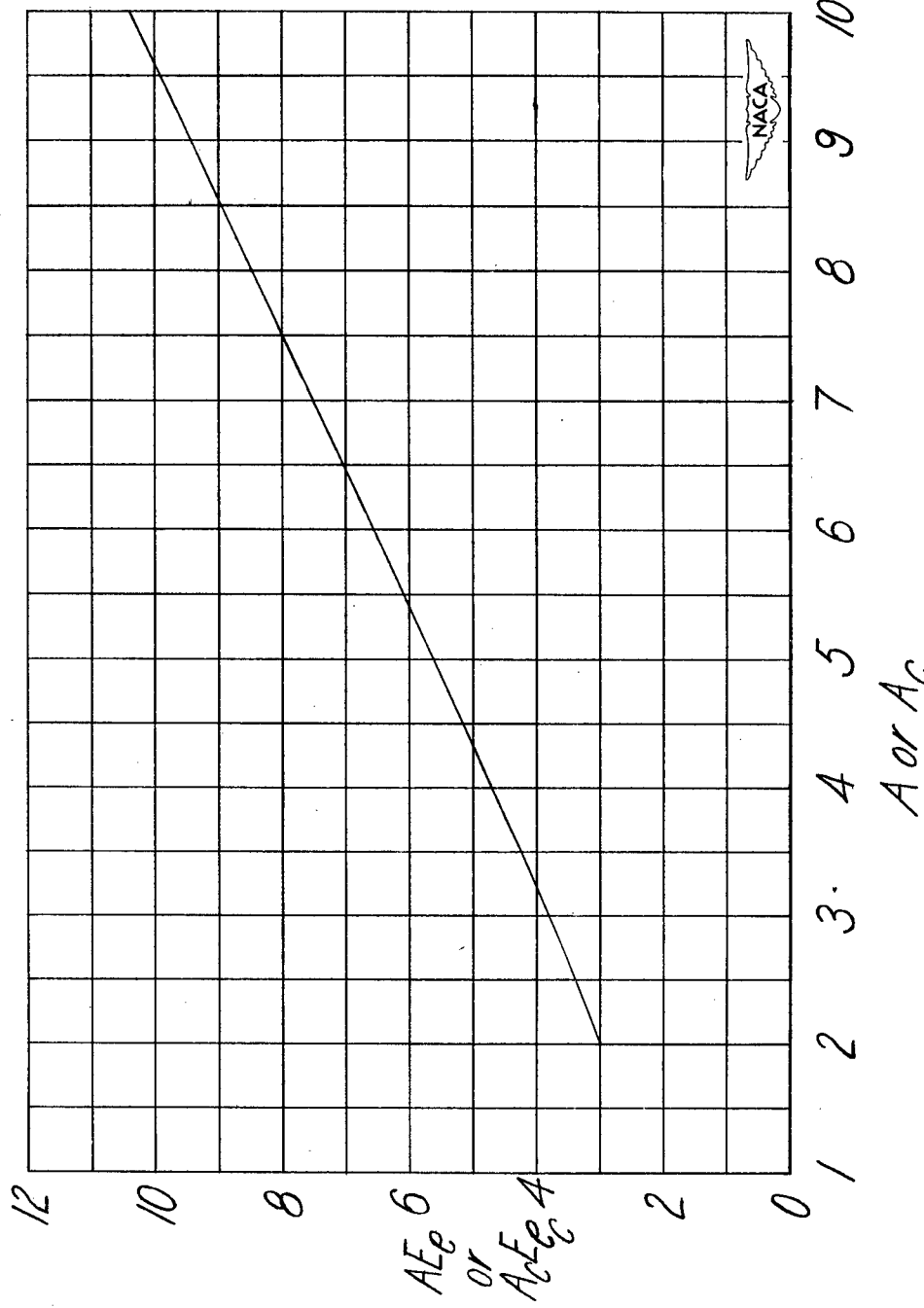


Figure 4 - Quantity useful for evaluation of the lift-curve slope by lifting-surface theory (reference 6).

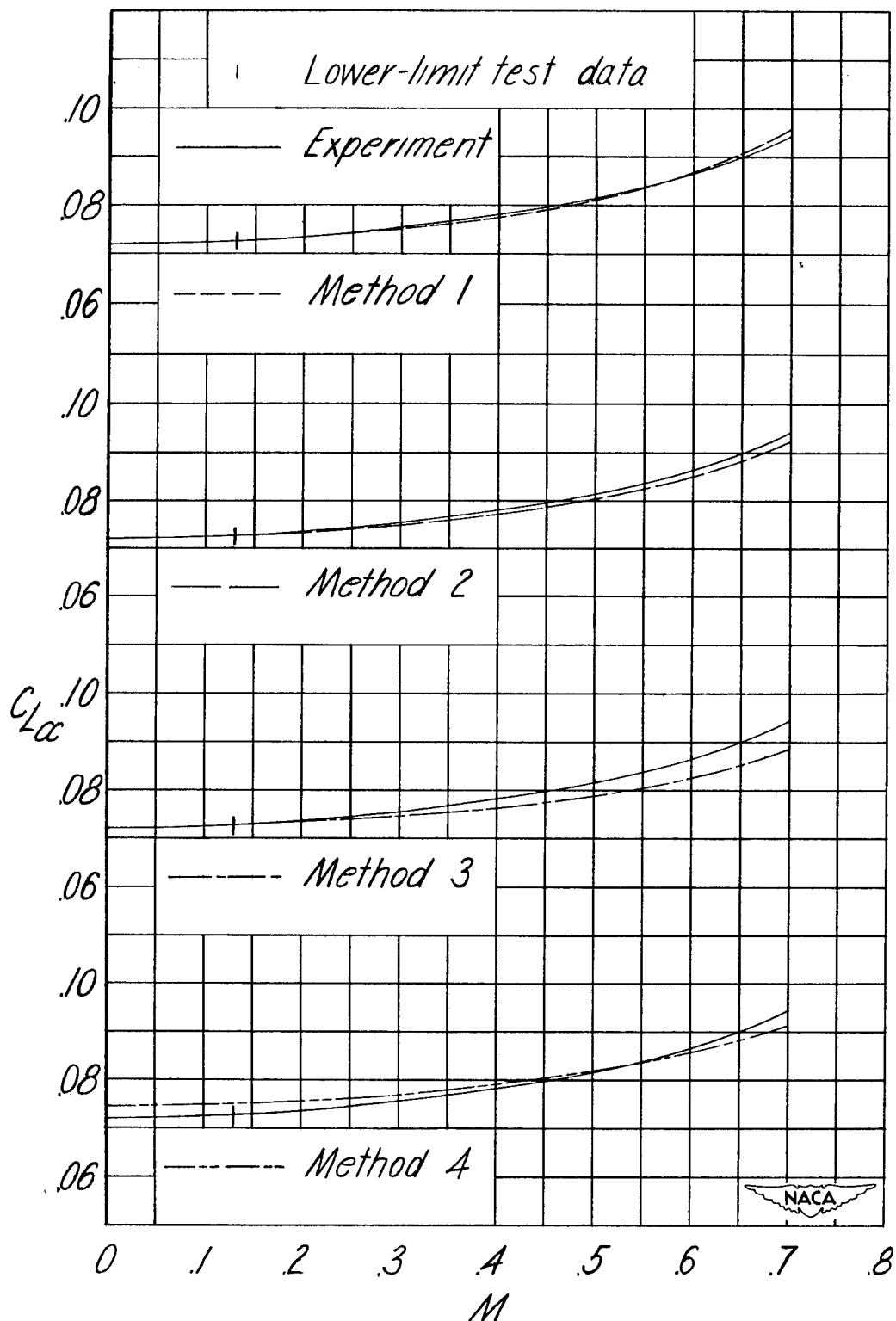


Figure 5.- Variation of lift-curve slope with Mach number. $\Lambda = 0^\circ$. Model 4.

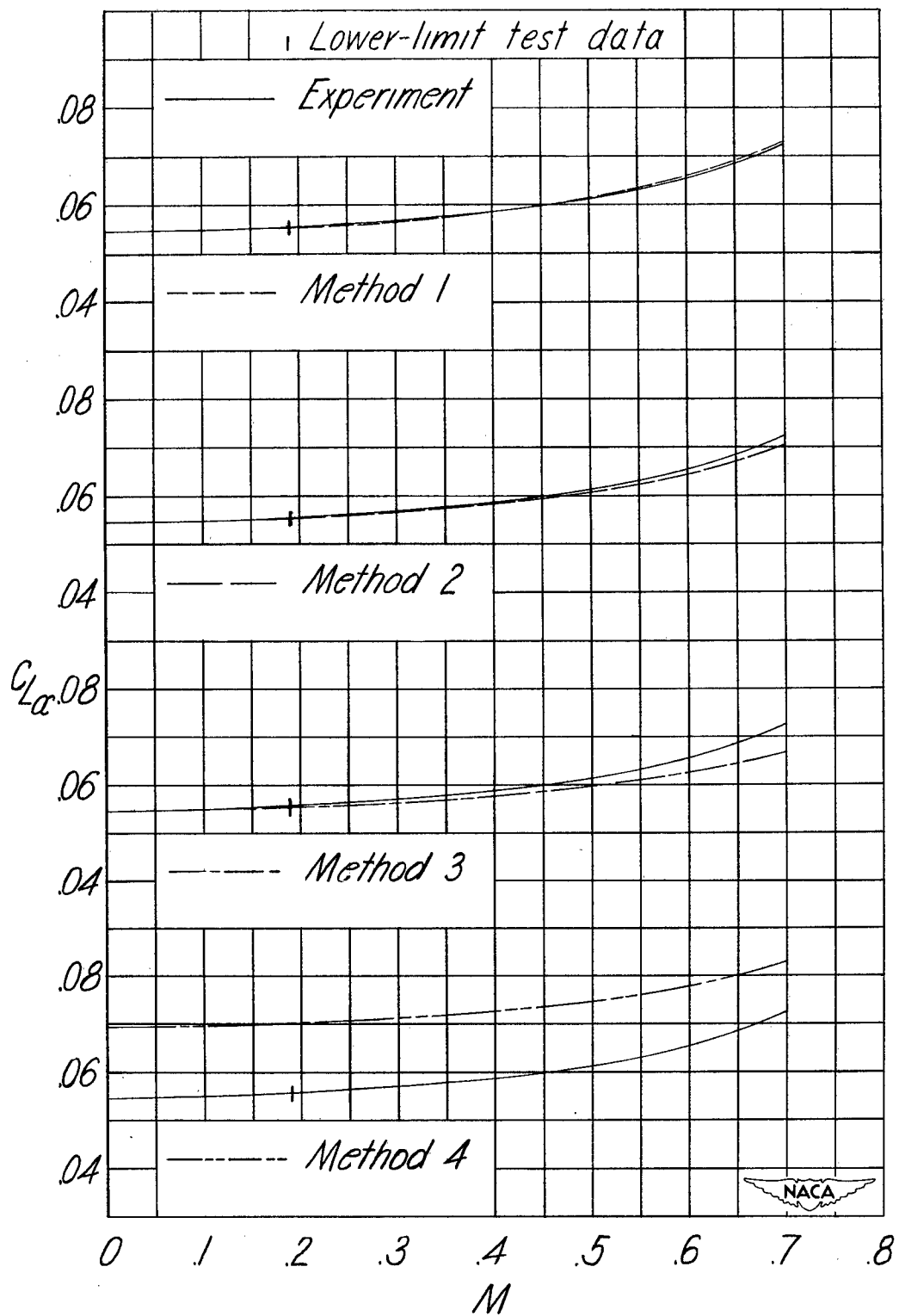


Figure 6.- Variation of lift-curve slope with Mach number. $\Lambda = 8^\circ$. Model 5.

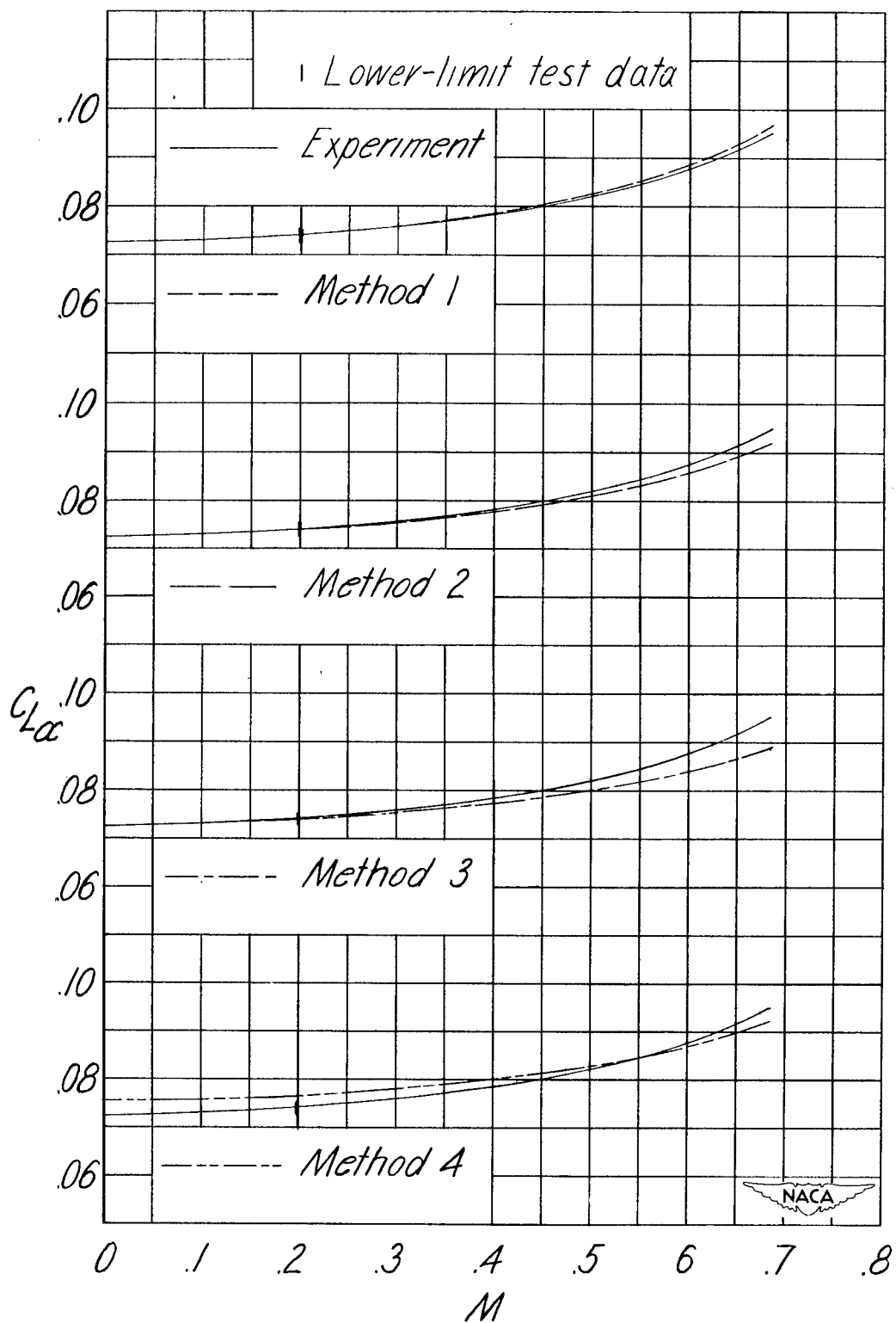


Figure 7.- Variation of lift-curve slope with Mach number. $\Lambda = 0^\circ$. Model 6.

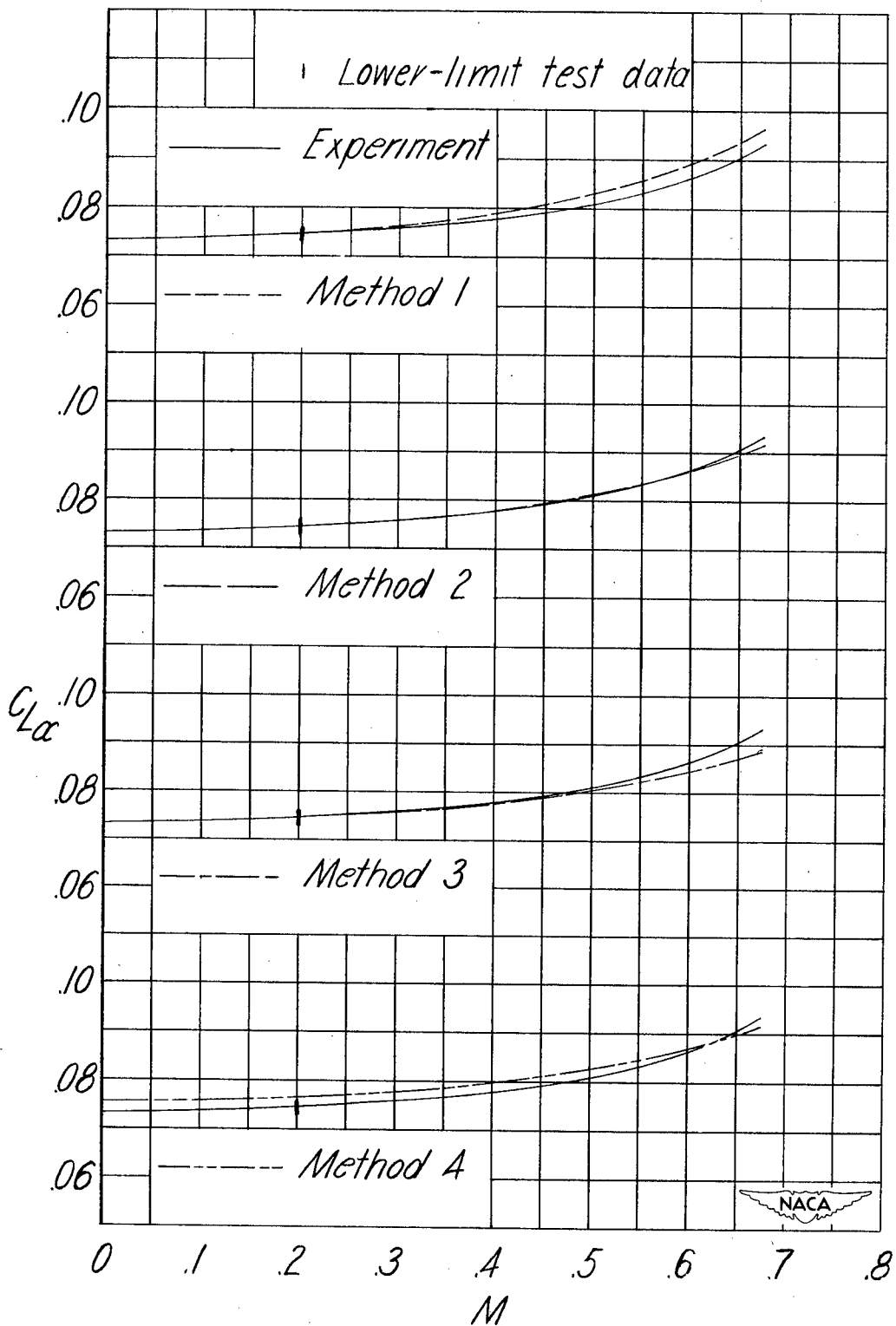


Figure 8.- Variation of lift-curve slope with Mach number. $\Lambda = 3.2^\circ$. Model 7.

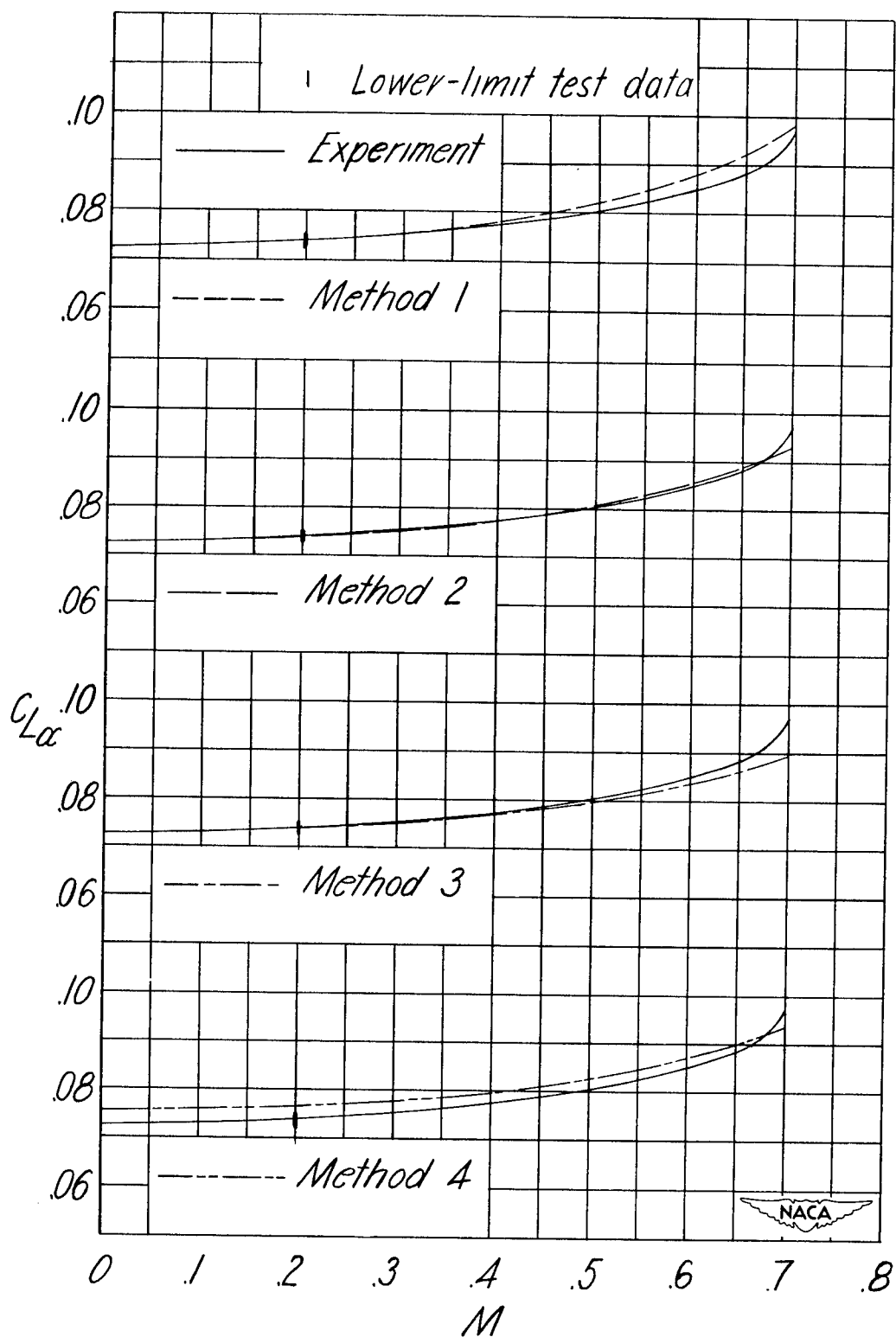


Figure 9.- Variation of lift-curve slope with Mach number. $\Lambda = 3.2^\circ$. Model 8.

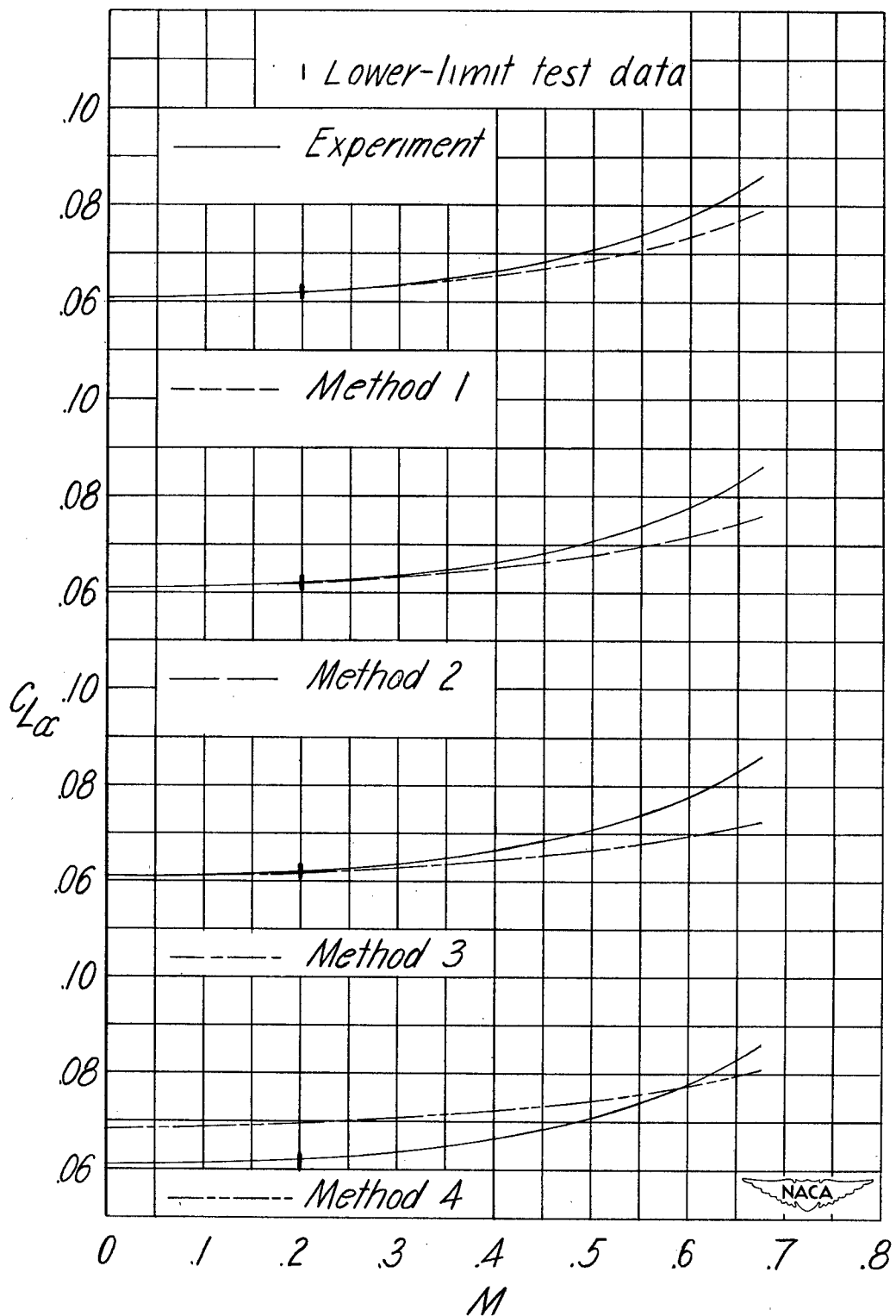


Figure 10.- Variation of lift-curve slope with Mach number. $\alpha = 6.3^\circ$. Model 9.

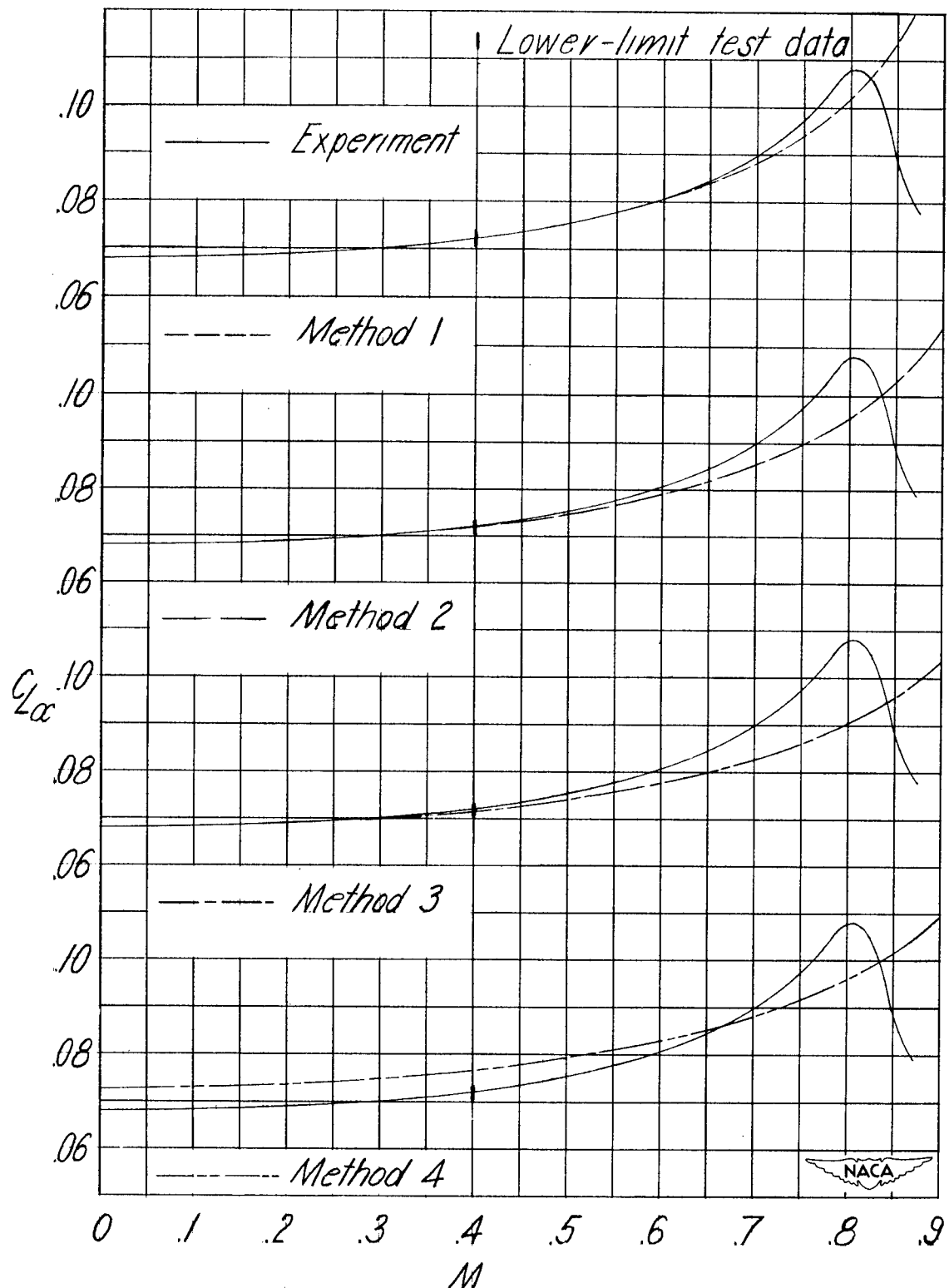


Figure 11.- Variation of lift-curve slope with Mach number. $\Lambda = 11.5^\circ$. Model 10.

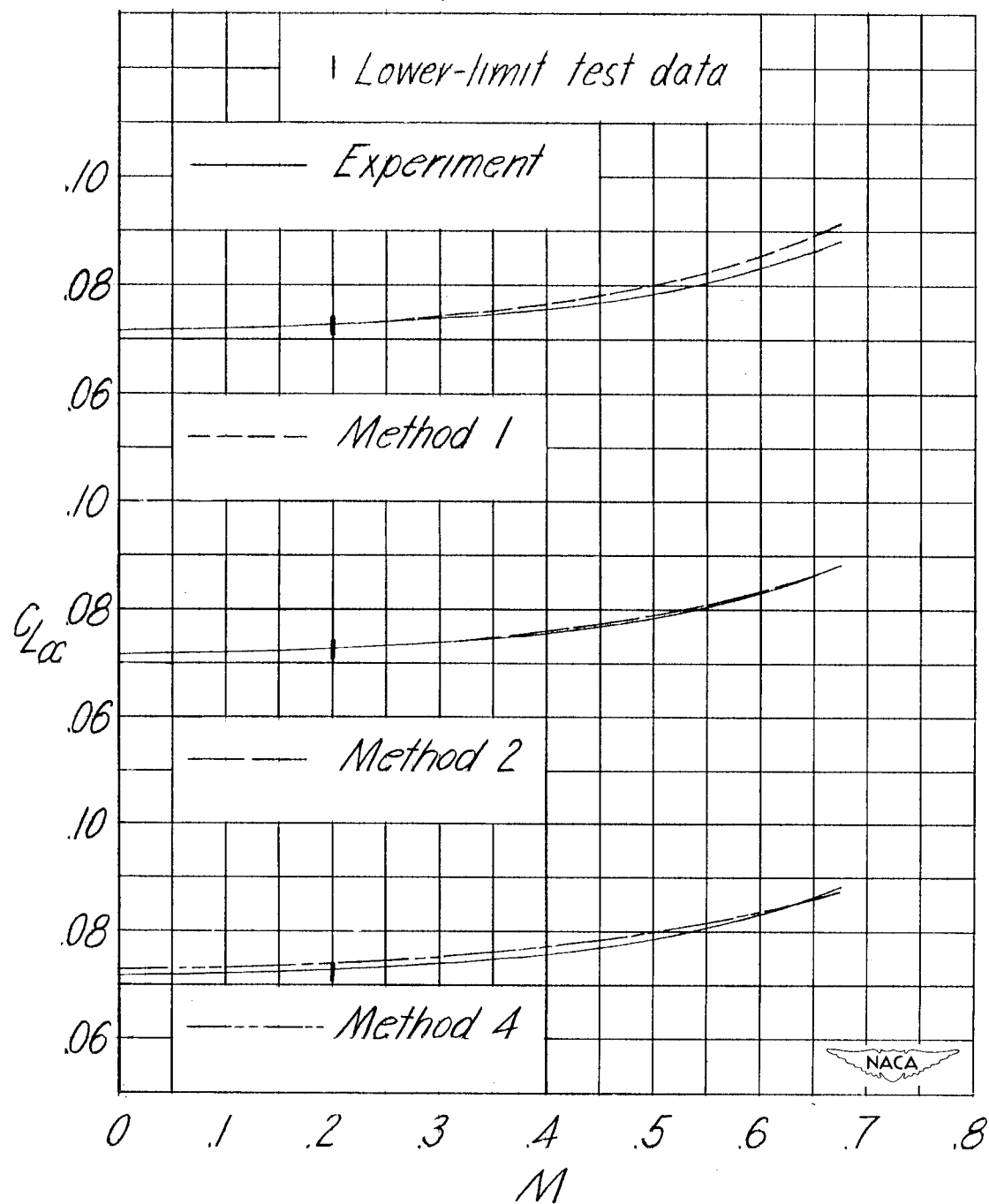


Figure 12.- Variation of lift-curve slope with Mach number. $\Lambda = 15.0^\circ$. Model 11.

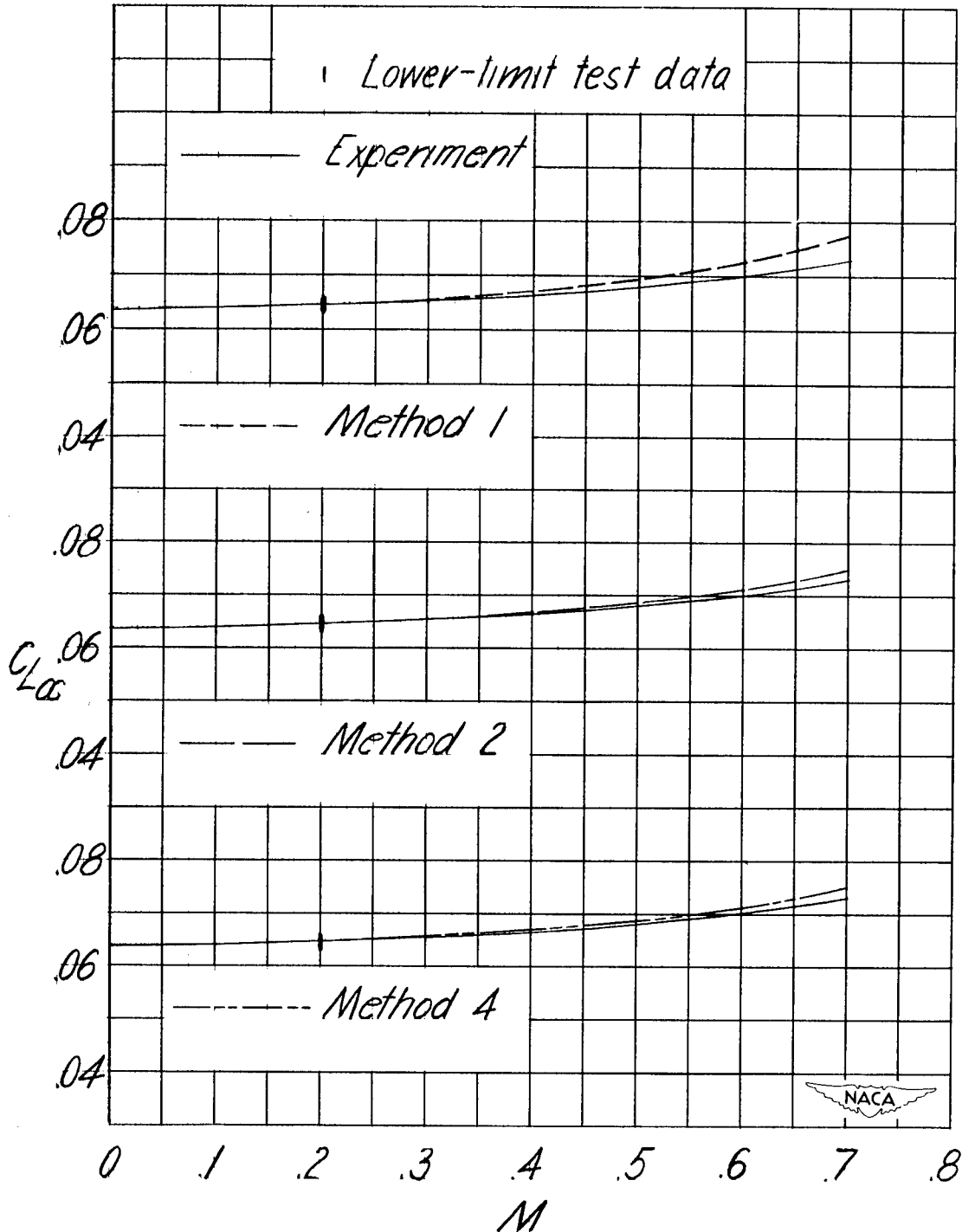


Figure 13.- Variation of lift-curve slope with Mach number. $\Lambda = 30.0^\circ$. Model 12.

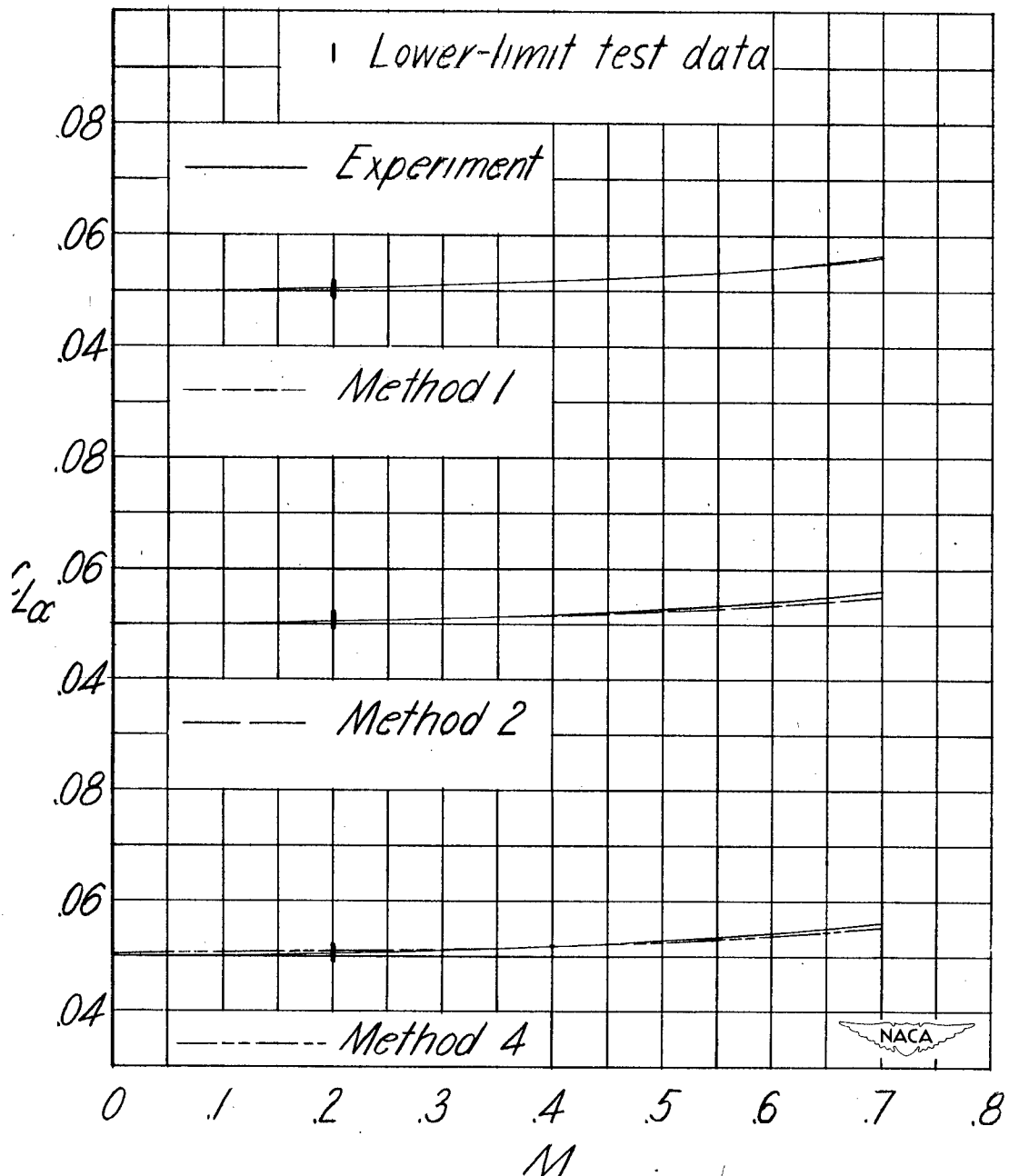


Figure 14.- Variation of lift-curve slope with Mach number. $\Lambda = 45.0^\circ$. Model 13.

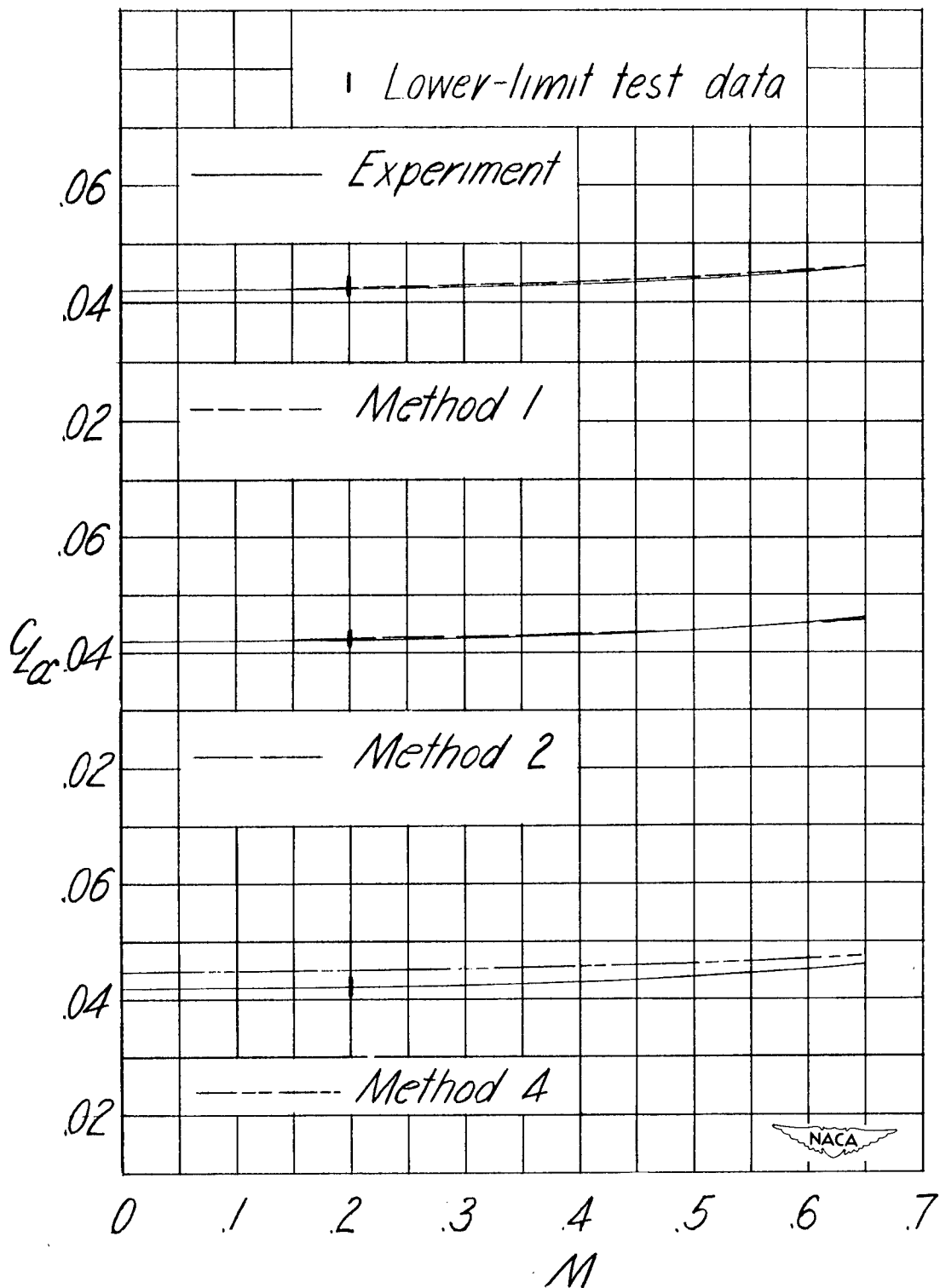


Figure 15.- Variation of lift-curve slope with
Mach number. $\Lambda = -45.0^\circ$. Model 1A.

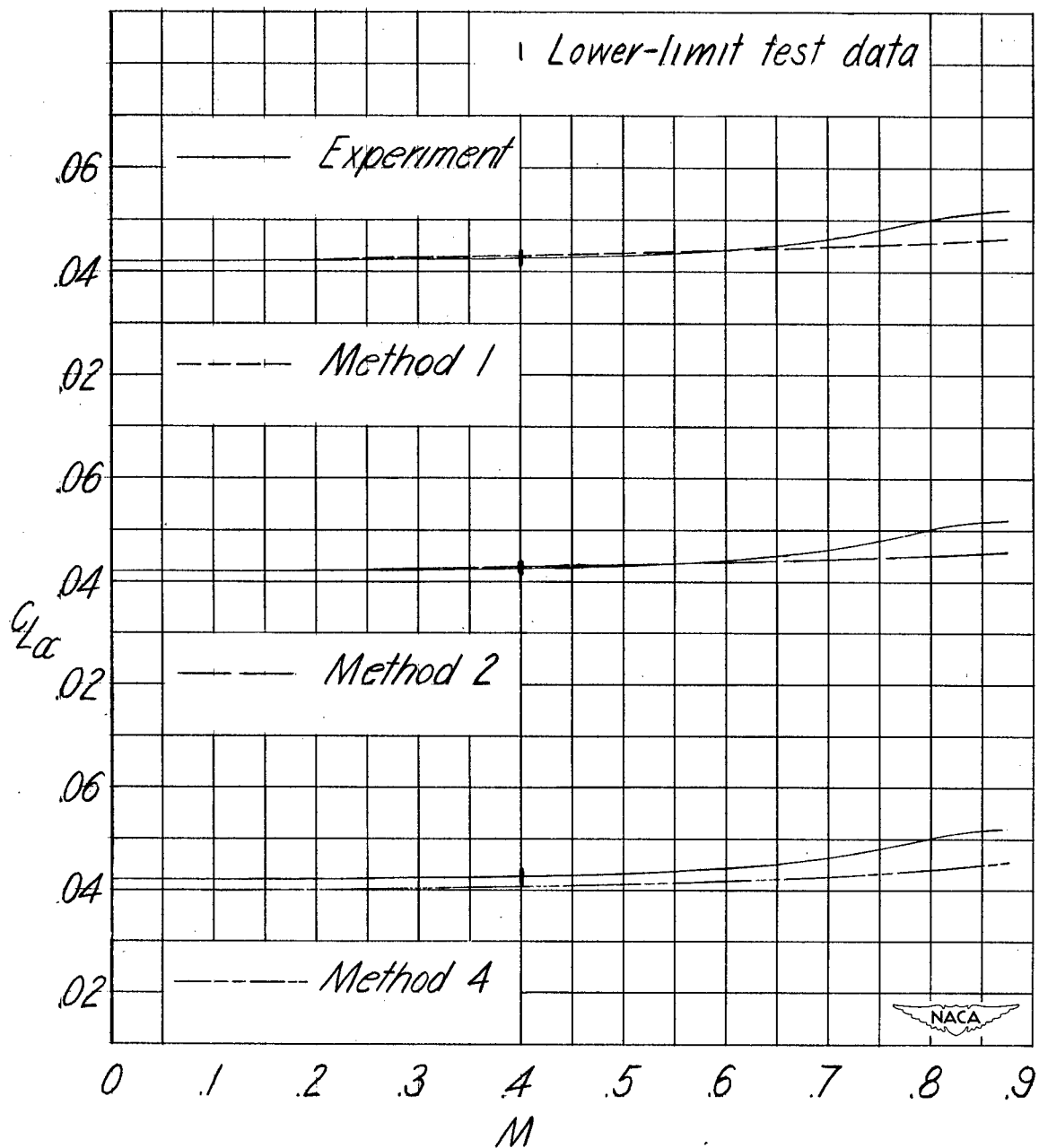


Figure 16.- Variation of lift-curve slope with Mach number. $\Lambda = 56.5^\circ$. Model 15.

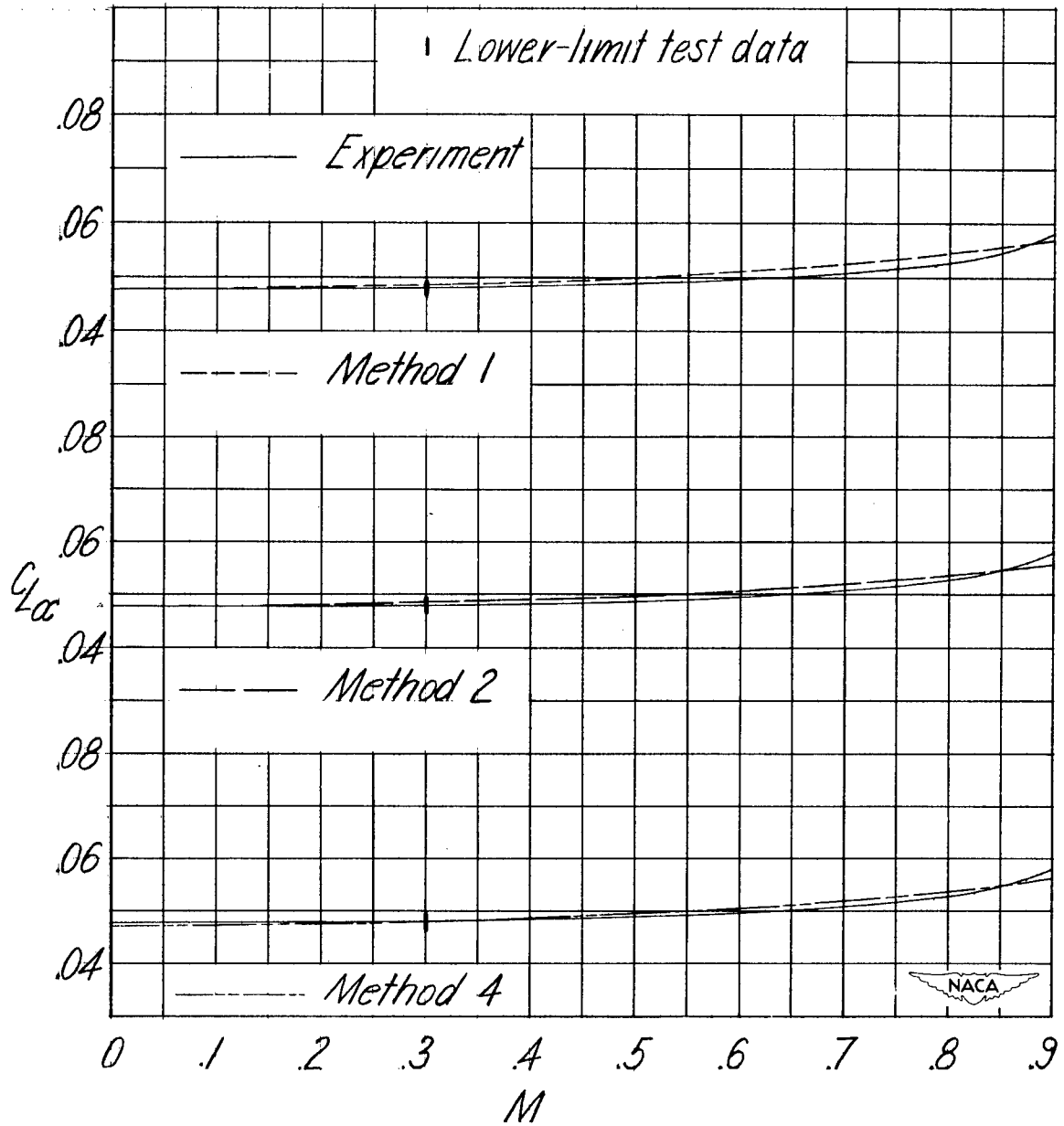


Figure 17.- Variation of lift-curve slope with Mach number. $\Lambda=47.8^\circ$. Model 16.

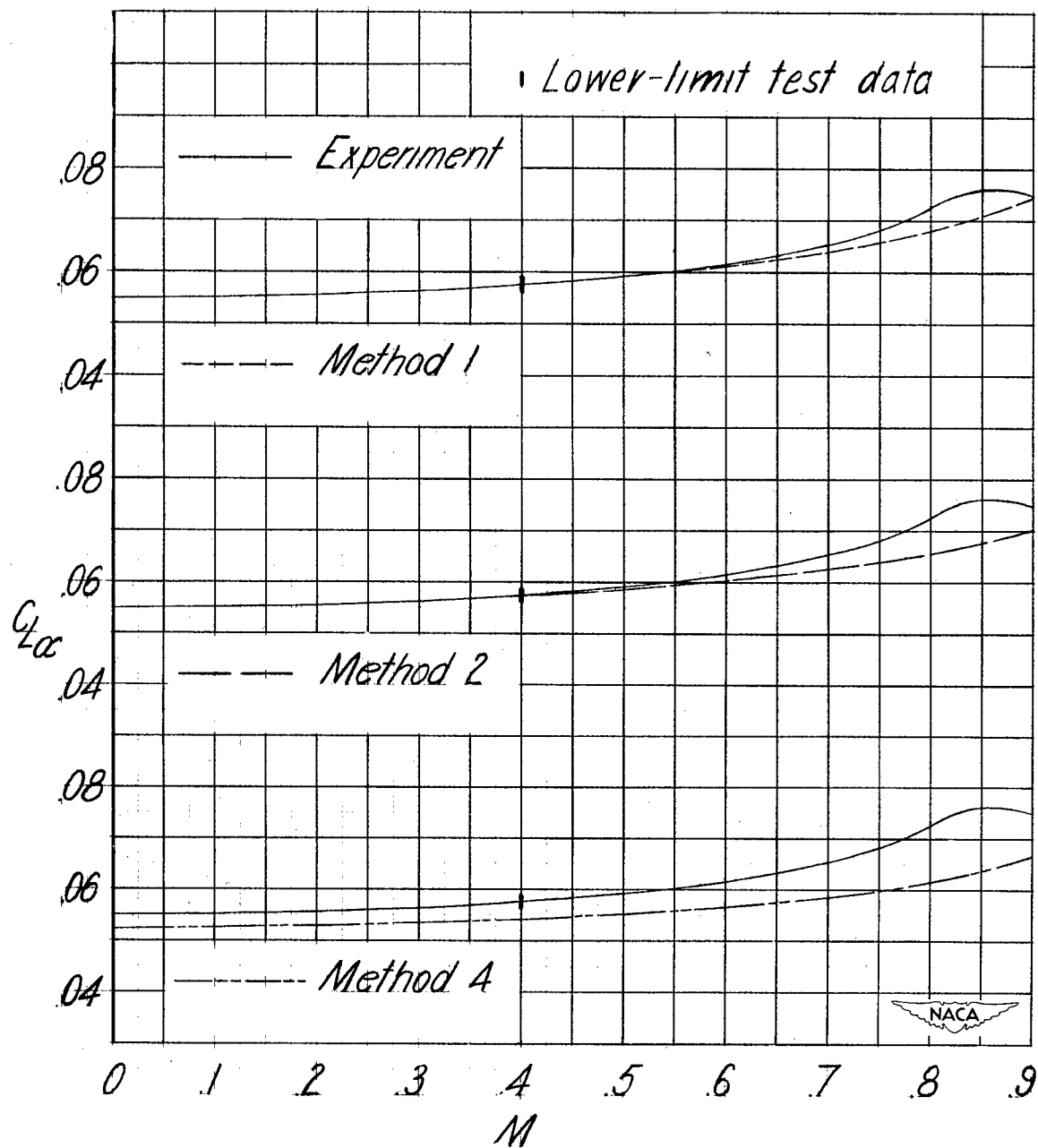


Figure 18.- Variation of lift-curve slope with Mach number. $\Lambda = 35.0^\circ$. Model 17.

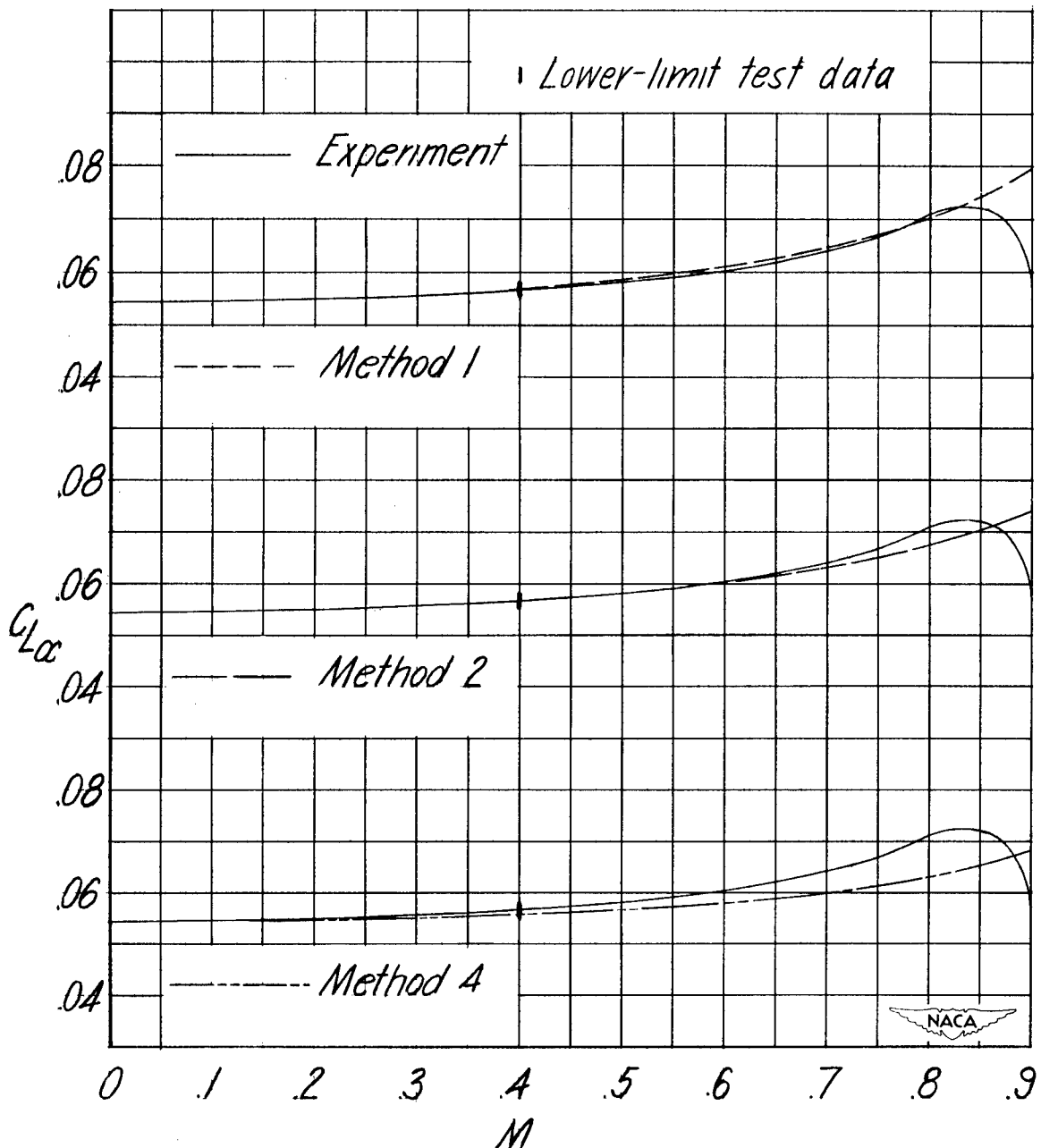


Figure 19.- Variation of lift-curve slope with Mach number. $\Lambda = 27.5^\circ$. Model 18.

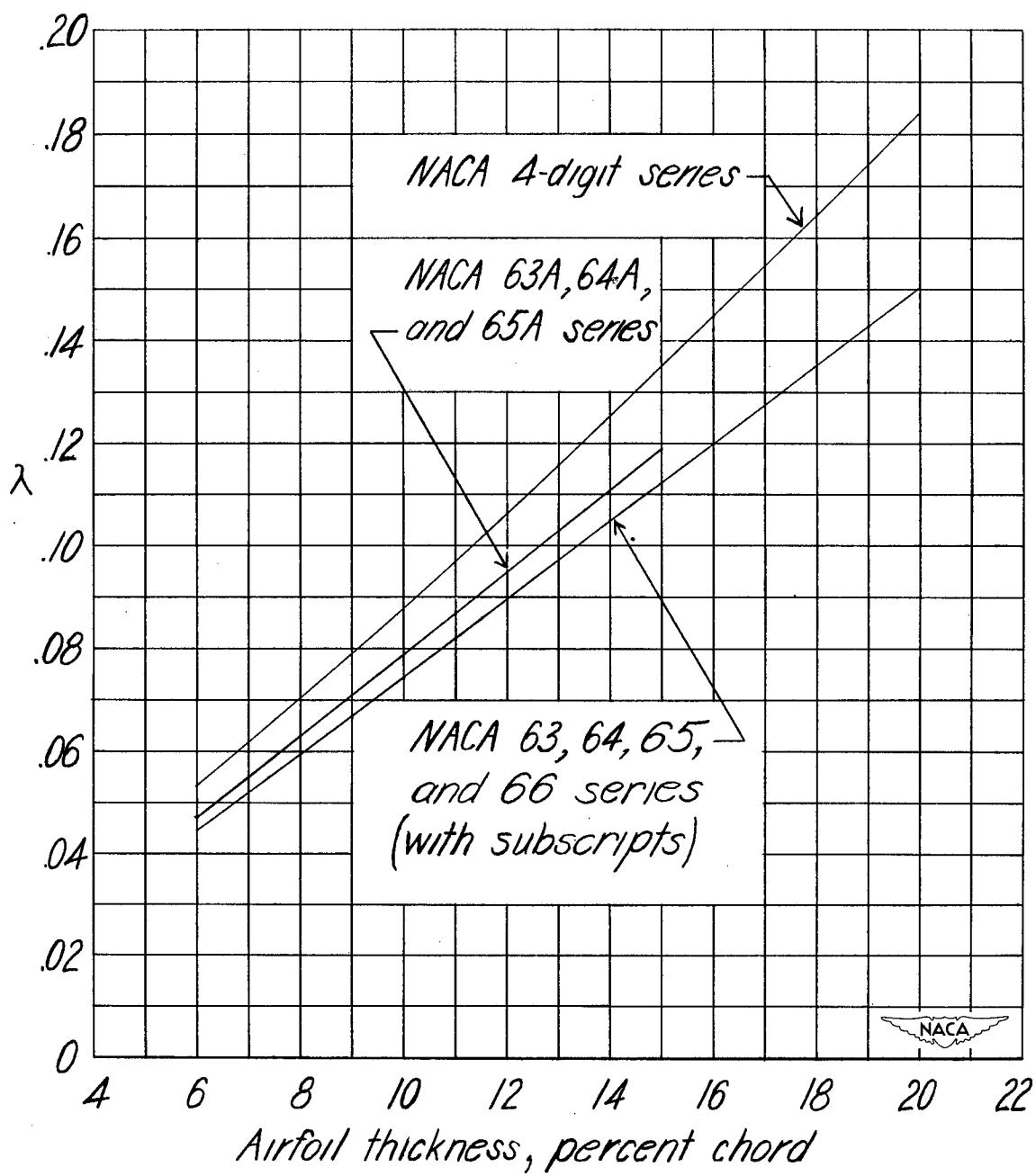


Figure 20.-Variation with airfoil thickness of the airfoil-thickness parameter for several series of NACA airfoils.